American Mineralogist, Volume 83, pages 881–888, 1998

Synthesis, crystal structure, and phase relations of $AlSiO_3OH$, a high-pressure hydrous phase

Max W. Schmidt,[1,*] Larry W. Finger,[2] Ross J. Angel,[3] and Robert E. Dinnebier[4]

[1]CNRS-UMR 6524, Magmas et Volcans, 5 rue Kessler, 63038 Clermont-Ferrand, France
[2]Bayerisches Geoinstitut, 95440 Bayreuth, Germany, and Geophysical Laboratory and Center for High Pressure Research, 5251 Broad Branch Road, N.W., Washington, D.C. 20015, U.S.A.
[3]Bayerisches Geoinstitut, 95440 Bayreuth, Germany
[4]Lehrstuhl für Kristallographie, Universität Bayreuth, 95440 Bayreuth, Germany

Abstract

Phase egg, first described by Eggleton et al. (1978), was synthesized and its composition determined to be $AlSiO_3OH$. The crystal structure of $AlSiO_3OH$, including the position of the hydrogen, has been solved and refined from high-resolution X-ray powder diffraction. The resulting lattice constants are $a = 7.14409(2)$ Å, $b = 4.33462(1)$ Å, $c = 6.95253(2)$ Å, and $\beta = 98.396(1)°$. The space group is $P2_1/n$; $Z = 4$, $V_0 = 212.99(1)$ Å^3, and the zero pressure density is 3.74 g/cm^3. This phase, which has features in common with the stishovite structure, occurs above 11 GPa and 700 °C. $AlSiO_3OH$ forms from topaz-OH with increasing pressure and persists to more than 17.7 GPa and 1300 °C. From a Schreinemaker analysis, we predicted that phase egg decomposes with pressure to an unknown, possibly hydrous aluminosilicate. Potentially, phase egg could replace topaz-OH or kyanite in subducted crustal bulk compositions and may transport some water into the deep Earth.

Introduction

The structure and stability of hydrous high-pressure phases have received considerable attention recently because of their importance in many geodynamical processes. Attention has been focused on the MgO-SiO_2-H_2O system, which is directly applicable to the Earth's mantle, and also the Al_2O_3-SiO_2-H_2O system. In the later system, kaolinite and pyrophyllite constitute stable phases at crustal conditions. Toward higher pressures, initially phase Pi = $Al_3Si_2O_7(OH)_3$ (Coes 1962; Wunder et al. 1993a) and then topaz-OH = $Al_2SiO_4(OH)_2$ (Wunder et al. 1993b) form in water-saturated systems. At higher pressures, Eggleton et al. (1978) was the first to synthesize a hydrous phase with Al:Si = 1:1. This study investigates the structure and composition of this high-pressure phase, which has been termed ''phase egg'' (Schmidt 1995). Additional experiments, combined with results obtained from the literature, allow the delineation of the stability relations of topaz-OH and phase egg.

Synthesis

Starting materials were prepared from cristobalite, Al_2O_3, and $Al(OH)_3$. Because the water content of phase egg could not be directly measured, much effort was put to constrain the water content as closely as possible during syntheses. The use of $Al(OH)_3$ permits the addition of precise quantities of H_2O to the starting material. SiO_2 and Al_2O_3 were fired at 1200 °C, and $Al(OH)_3$ was dried at 110 °C prior to mixing. The exact water content of $Al(OH)_3$ was determined by firing to 900 °C and measuring the weight loss. Dehydration was complete at 450 °C, the weight loss of $Al(OH)_3$ between 110 and 450 °C being almost exactly equivalent to its stoichiometric water content of 34.6 wt%. For synthesis, two starting materials were prepared with Al:Si ratios of 1:1 and water contents of 7.8 and 7.2 wt%. The prepared starting materials were stored in a desiccator and dried again at 100 °C just before loading the capsules, which were immediately welded. During the welding, the lower end of the capsule was cooled with water to ensure that temperatures within the capsule did not exceed 100 °C. Only capsules that could be welded during the first attempt were used.

Experiments were conducted in a split sphere multianvil (MA-8) device employing prefabricated MgO-octahedra with an edge length of 14 mm on WC-cubes of 32 mm edge length with a truncation edge length of 8 mm. Gaskets were made from natural pyrophyllite. A stepped $LaCrO_3$-furnace inside a ZrO_2-sleeve was used as heater. Capsules were separated from the furnace by a MgO-sleeve (Rubie et al. 1993; Schmidt 1995). Temperature was read by a Pt-$Pt_{10}Rh_{90}$ S-type thermocouple, which was not corrected for the effect of pressure on the thermocouple emf. Capsules were made of 1.6 mm O.D. platinum tubing and had initial lengths of 2.7 mm, equivalent to the length of the central thickened part of the heater. Temperature gradients over the capsule length were less than 60 °C and thermocouple readings represent essentially the coldest temperature within the capsule. Pressure

* E-mail: max@opgc.univ-bpclermont.fr

TABLE 1. Averaged EMP analyses of phase egg

Experiment	lwma37	lwma40	lwma20	lnwm220
No. of analyses	9	8	6	Std. dev.
		Weight percent		
SiO_2	50.72	50.49	49.84	0.59
Al_2O_3	41.38	42.13	41.84	0.47
CaO	—	—	0.06	0.04
Total	92.10	92.62	91.74	0.64
H_2O*	7.48	7.51	7.44	
Total*	99.58	100.13	99.18	
Si	1.017	1.007	1.004	0.009
Al	0.978	0.991	0.994	0.012
Ca	—	—	0.001	0.001
H*	1.000	1.000	1.000	

Note: Experiment lwma20 from Schmidt (1995).
* H_2O contents calculated on the basis of Al : Si : H = 1:1:1, see text.

was calibrated against coesite-stishovite (Zhang et al. 1996) and α-β Mg_2SiO_4 transitions (Katsura and Ito 1989) and is believed to be accurate to ±4%.

COMPOSITION OF PHASE EGG

Scanning electron microscopy revealed that experimental products contained texturally equilibrated polycrystalline aggregates with grain boundaries meeting at 120° angles. Thus we could not identify the proper habit of phase egg. Typical grain sizes were between 2 and 4 μm, only few grains were larger (up to 10–12 μm). Compositions of experimental products were measured from three experiments by electron microprobe (EMP) using a beam of 12 kV, 20 nA. Standards were quartz, corundum, and wollastonite (the latter for analysis of experiment lwma20 from Schmidt (1995) in a CaO-Al_2O_3-SiO_2-H_2O-system). Analysis of phase egg produced in both the CASH and the ASH systems yielded Al:Si ratios close to unity (Table 1), in agreement with the original study of Eggleton et al. (1978). The solubility of CaO in phase egg appears to be low, a maximum content of 0.18 wt% CaO was measured, the average being 0.06 wt% CaO. Totals of all analyses for phase egg averaged 92.2 ± 0.6 wt% (Table 1). The same polished sections yielded totals of 99.6–100.8 wt% for kyanite, stishovite, corundum, and grossular. Thus, the H_2O content of phase egg is likely 7.8 ± 0.6 wt%.

The H_2O content of phase egg is also indicated from the bulk compositions used for synthesis: experiment lwma70 (Table 2) with 7.8 ± 0.1 wt% H_2O (Al:Si:H = 1:1:1.04) resulted in >90% phase egg with stishovite + diaspore. Opening the capsule revealed a humid white powder, indicating the presence of an excess fluid phase. Phase egg + stishovite + diaspore are co-linear (Fig. 1) and thus do not have a stability field in a three component system. From the diffraction profiles, we believe that diaspore has precipitated upon quench from the excess fluid phase. An assemblage deficient in water with respect to phase egg, experiment lwma37 with 7.2 ± 0.1 wt% H_2O (Al:Si:H = 1:1:0.98), resulted in >90% phase egg with stishovite + corundum as excess phases. The powder appeared to be dry, however, no further attempt was made to detect small quantities of water.

TABLE 2. Experimental conditions for synthesis experiments

Exper. name	*P* (GPa)	*T* (°C)	Time (min)	Solid experimental products
lwma37	14.0	1000	270	egg, cor, st
lwma40	13.5	1100	570	egg, ky, st
lwma62	11.3	800	90	toz, cor, st, dia
lwma70	15.0	1000	240	egg, dia, st

Note: cor = corundum, dia = diaspore, egg = $AlSiO_3OH$ = phase egg, ky = kyanite, st = stishovite, toz = topaz-OH.

The combined electron microprobe analyses and bulk compositions for synthesis implicate 7.6 ± 0.4 wt% as the water content of phase egg. As described later, the unit cell of phase egg contains 4 Al and 4 Si atoms. For an Al:Si:H ratio of 1:1:1, the ideal formula of phase egg is $AlSiO_3OH$ and has a stoichiometric water content of 7.50 wt%. Newby ratios of Si:Al:H = 4:4:3 or 4:4:5 require water contents of 5.7 and 9.2 wt%, respectively, which are beyond the limits imposed by synthesis compositions and microprobe analyses.

STRUCTURE DETERMINATION AND REFINEMENT

Diffraction patterns for all experiments were obtained with a SIEMENS D5000 powder diffractometer with flat-plate geometry. The sample that appeared to have the lowest impurity content (lwma70) was selected for high-resolution diffractometry on BM16 (beamline 15) at the European Synchrotron Research Facility (ESRF), Grenoble, France. This instrument consists of nine detectors separated by 2°, each with a Ge(111) analyzer crystal. The optimal instrument contribution to the peak width is 0.002°, which is obtained through the use of a vertically collimating mirror before a Si(311) double-crystal monochromator, therefore, the highest possible resolution can be obtained on this beamline.

The sample was placed in a capillary with an inside diameter of 0.5 mm and spun about the cylindrical axis

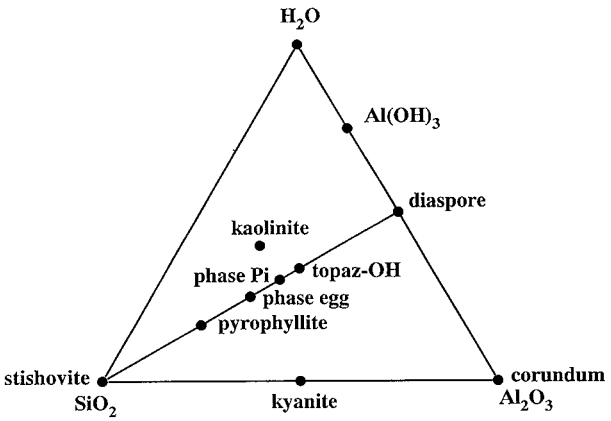

FIGURE 1. The system Al_2O_3-SiO_2H_2O showing the phases of interest in this study.

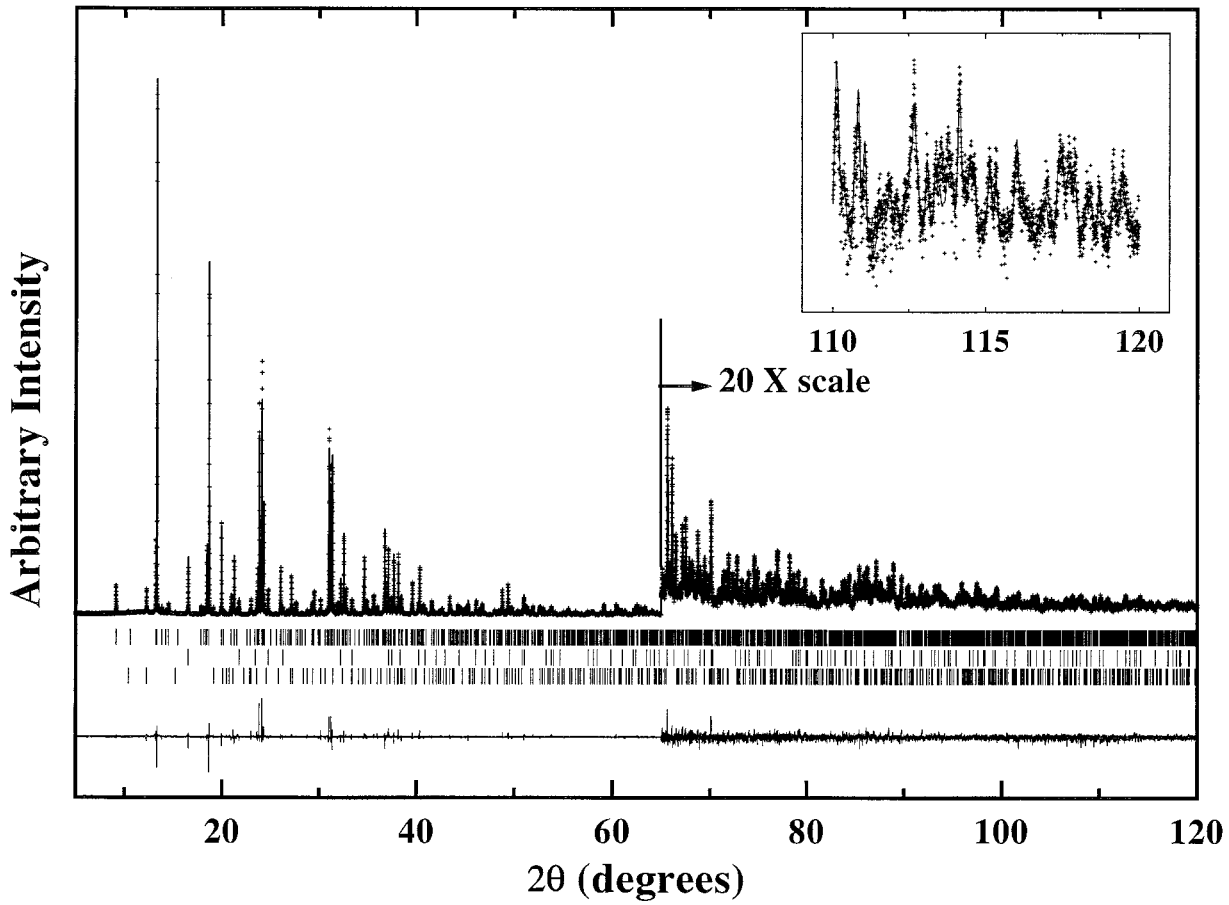

FIGURE 2. Results of Rietveld refinement on the powder pattern measured in this study at a wavelength of 0.84933 Å. The upper solid line shows the calculated reflection envelope, and the plus signs are the observed data. The difference function is represented by the lower solid line. From top to bottom, the vertical ticks represent the locations of reflections for $AlSiO_3OH$, stishovite, and diaspore, respectively. The inset shows the region from 110 to 120° 2θ with a greatly expanded vertical scale. This highly crystalline sample diffracts even at a resolution of 0.49 Å.

during data collection. In this instrument, the 2θ axis is driven continuously, and the data accumulated by sampling the detectors and 2θ encoder with a frequency between 50 and 100 Hz, depending upon scan speed. The resulting data are stored, but the detectors are not cleared. In later processing, data from the nine channels are corrected and summed, and the data are rebinned to form a pseudo step-scan data set. In this experiment, an initial scan of 2 °/min for the center detector between −2 and 140° was followed by subsequent scans of 2 °/min from −2 to 38°, 1 °/min from 38 to 68°, 0.5 °/min from 68 to 88°, and 0.25 °/min from 88 to 118°. After rebinning to a constant step size of 0.004°, a total of 39 472 data steps were obtained. Of these, the 28 750 between 5 and 120° were used in further calculations. The wavelength for this experiment was determined from a Si standard to be 0.84933(1) Å, thus the resolution of the pattern is 0.49 Å. Significant peaks occur even at this very high diffraction angle (Fig. 2).

Individual peaks to 1.3 Å were extracted from the pattern to check the previous phase identifications and to determine initial profile parameters. The diffractometer uses a detector opening of nearly 10 mm, and a sample illumination length of 4.5 mm, therefore, there is considerable asymmetry for low-angle peaks due to axial-divergence. Accordingly, the peak profiles and positions were corrected for asymmetry using the method of Finger et al. (1994). The resulting peaks had three distinct widths, confirming that the sample consists of three phases—stishovite, diaspore, and phase egg. All 52 *d* spacings for the latter material could be indexed by program TREOR (Werner et al. 1985) with a monoclinic cell. Figures of merit are M(20) = 117 (de Wolff 1968) and F20 = 182 (Smith and Snyder 1979), leaving no doubt as to the correctness of the indexing. Systematic absences are consistent with space group $P2_1/n$. Table 3 compares the spacings and intensities for this study with those of Eggleton et al. (1978), who misindexed the pattern, mainly because three extra peaks from diaspore were thought to belong to this phase. The unit cell obtained from the

TABLE 3. Comparison of diffraction patterns for $AlSiO_3OH$

	This study			Eggleton et al. (1978)*	
hkl	*d* (calc)	*d* (obs)	*I*	*d*	*I*
$10\bar{1}$	5.3339	5.3295	6	5.34	50
110	3.6949	3.6945	13		
011	3.6670	3.6665	100	3.67	100
200	3.5338	3.5334	1	3.54	10
$00\bar{2}$	3.4390		<1	3.44	10
$11\bar{1}$	3.3638	3.3633	2	3.36	20
210	2.7390	2.7386	1	2.74	10
$01\bar{2}$	2.6941	2.6938	1	2.695	10
$21\bar{1}$	2.6497	2.6495	13	2.649	40
$11\bar{2}$	2.6190	2.6188	67	2.616	100
211	2.4511	2.4509	16	2.450	70
$11\bar{1}$	2.4267	2.4264	<1		
$30\bar{1}$	2.3358	2.3356	3	2.334	30
$20\bar{2}$	2.3022	2.3029	10	2.301	60
$10\bar{3}$	2.2807	2.2805	1		
120	2.0721	2.0716	2		
310	2.0699	2.0696	8		
$02\bar{1}$	2.0671	2.0670	<1		
$31\bar{1}$	2.0562	2.0561	39	2.054	90
212	2.0333	2.0331	46	2.031	100
$01\bar{3}$	2.0267	2.0265	3		
$11\bar{3}$	2.0184	2.0182	25	2.014	60
$31\bar{2}$	1.8834	1.8833	9	1.881	60
$21\bar{3}$	1.8650	1.8648	<1		
220	1.8475	1.8474	<1		
$02\bar{2}$	1.8336	1.8334	<1	1.832	10
$22\bar{1}$	1.8194	1.8193	<1		
$12\bar{2}$	1.8094	1.8092	8	1.807	60
$30\bar{3}$	1.7779	1.7778	2	1.775	30
400	1.7669	1.7666	<1		
221	1.7510	1.7508	<1		
$12\bar{2}$	1.7421	1.7421	<1		
$22\bar{2}$	1.6819	1.6820	<1		
$31\bar{2}$	1.6807	1.6806	2		
$40\bar{2}$	1.6741	1.6740	<1	1.678	20
$21\bar{3}$	1.6676	1.6675	5	1.666	40
$20\bar{4}$	1.6435	1.6432	<1	1.641	10
$32\bar{0}$	1.5959	1.5949	<1		
$32\bar{1}$	1.5887	1.5886	33	1.587	100
$22\bar{2}$	1.5781	1.5780	26	1.574	90
$12\bar{3}$	1.5711	1.5710	32	1.570	100
411	1.5454	1.5453	2	1.544	20
303	1.5367	1.5365	<1		
114	1.5153	1.5152	17	1.514	70
$12\bar{3}$	1.5055	—	2		
$32\bar{2}$	1.5048	1.5050	4	1.502	20
402	1.4859	1.4857	<1		
$20\bar{4}$	1.4643	1.4642	<1		
$41\bar{3}$	1.4261	1.4260	11	1.425	60
$31\bar{4}$	1.4149	1.4150	2		
$03\bar{1}$	1.4140	1.4142	1	1.413	30
$13\bar{1}$	1.3946	1.3943	1		
$10\bar{5}$	1.3889	1.3988	1		
$22\bar{3}$	1.3877	1.3874	3	1.387	40
$42\bar{1}$	1.3732	1.3737	<1	1.372	100
501	1.3464	1.3460	16	1.346	80
$51\bar{0}$	1.3439	1.3436	5		
$40\bar{4}$	1.3334	1.3332	14		
$13\bar{2}$	1.3227	1.3224	3	1.322	20
$51\bar{2}$	1.3151		1		
$10\bar{5}$	1.3148	1.3145	11	1.314	60
$22\bar{4}$	1.3096		1		
231	1.2994	1.2992	10	1.298	50

* Lines seen by Eggleton et al. at $d = 3.98$ and 2129 (both with $I = 30$) and $d = 1.630$ with $I = 10$ belong to diaspore.

high-resolution data is the same as found for the laboratory instrument, however, in the latter case the figures of merit were too small for us to be confident of the results.

To determine the structure, the Rietveld method was used to fit the pattern using the program GSAS (Larson and Von Dreele 1986). Intensity extraction was accomplished with the method of LeBail et al. (1988), with pseudo-Voigt peak profiles and the axial divergence asymmetry model of Finger et al. (1994). After convergence by refinement of a full set of instrumental parameters, the slope of the normal probability plot was 2.5, indicating a significant underestimation for the standard deviations of the intensities. After the previous sigmas were increased by this factor, the slope of the normal probability plot was changed to 1.02. At this stage $\chi^2_w = 1.4$. The peaks for diaspore were more than twice as broad as those for either stishovite or $AlSiO_3OH$. Structure factors for phase egg were then extracted and used as input to program SIRPOW (Altomare et al. 1994), a direct methods routine for intensities derived from a powder pattern. The initial experiment, using default parameter values yielded a solution. As expected, both Al and Si are octahedrally coordinated, and a preliminary assignment was based on average bond distance.

At this stage, all instrumental parameters were held fixed, and the initial atomic coordinates were refined with the Rietveld method. After convergence, the method of bond-valence sums (Brown 1992) was used to check the assignment of Al and Si and to determine the identity of the hydroxyl, and to determine which O atom is involved in the expected hydrogen bond. For the initial assignment of Al and Si, the valence sums were 3.14 and 3.96 for Al and Si, respectively. (If the assignment were reversed, the sums for Al and Si become 3.73 and 2.92, clearly incorrect.) For the correct allocation of Al and Si, the sums for the four O atoms are 1.93, 2.00, 1.66, and 1.27 for 01 to 04, respectively, implying that 04 is the hydroxyl, and 03 participates in a hydrogen bond.

After convergence, a difference electron density was computed. A peak with 0.8 e/Å^3 was found in the position expected for the H atom. This atom was added to the structural description and its position and temperature factor refined. The positions of H atoms have been inferred in previous experiments (Lengauer et al. 1995), but as far as we know, this is the first instance in which a H atom could be located and refined from X-ray powder data.

In the final refinement, lattice, profile, and background parameters were varied, along with the structural parameters for $AlSiO_3OH$. For stishovite and diaspore the intensities were matched with the LeBail et al. (1988) method—no structural model was used for these phases. The refinement converged to a reduced χ^2_w of 1.66. Residuals for the pattern are $R_{wp} = 0.112$, and $R_p = 0.087$. Bragg R values's for phase $AlSiO_3OH$ are $R(F^2) = 0.045$, $R(F) = 0.027$. The relatively large values for the profile residuals are due to the low background. Figure 2 shows the observed and calculated intensity data, and the difference between the two. Final values of atomic parameters are in Table 4; bond distances and angles are in Table 5.

The fundamental module of the structure, consists of edge-shared Si octahedra, linked to an Al_2O_{10} dimer (Fig.

TABLE 4. Refined atomic parameters for $AlSiO_3OH$

Atom	*x*	*y*	*z*	*B*
Al	0.06463(7)	0.02406(15)	0.70840(7)	0.270(8)
Si	0.68048(7)	0.01714(16)	0.58383(6)	0.314(7)
O1	0.1513 (2)	0.2023 (3)	0.2600 (3)	0.35 (2)
O2	0.5226 (2)	0.1937 (3)	0.3943 (2)	0.26 (2)
O3	0.88004(16)	0.2007 (3)	0.51236(17)	0.19 (1)
O4	0.76017(19)	0.2146 (3)	0.1288 (2)	0.31 (2)
H	0.796 (3)	0.553 (6)	0.422 (3)	1.7 (5)

Lattice constants: *a* 7.14409(2) Å; *b* 4.33462(1) Å; *c* 6.95253(2) Å; β 98.396(1)°; *V* 212.99(1) Å^3. Space group: $P2_1/n$. $z = 4$.

TABLE 5. Bond distances and angles for $AlSiO_3OH$

Bond distance (Å)		Angle (degree)	
Si-O1	1.7597(14)	O1-Si-O1	94.77(4)
Si-O1	1.7743(14)	O1-Si-O2	99.47(7)
Si-O2	1.7402(13)	O1-Si-O3	84.90(6)
Si-O2	1.7777(14)	O1-Si-O2	95.25(7)
Si-O3	1.7663(13)	O1-Si-O2	96.72(7)
Si-O4	2.0659(13)	O1-Si-O3	93.85(6)
Avg Si-O	1.8140	O2-Si-O2	81.04(7)
		O2-Si-O3	92.76(6)
		O2-Si-O4	85.25(6)
		O2-Si-O4	89.42(6)
		O3-Si-O4	80.00(6)
Al-O1	1.8679(14)	O1-Al-O2	92.55(7)
Al-O2	1.8358(14)	O1-Al-O3	78.41(6)
Al-O3	1.9076(12)	O1-Al-O3	95.62(6)
Al-O3	1.9126(13)	O1-Al-O4	97.42(6)
Al-O4	1.8720(15)	O2-Al-O3	93.92(7)
Al-O4	1.9410(13)	O2-Al-O4	96.08(6)
		O3-Al-O3	80.41(6)
Avg Al-O	1.8895	O3-Al-O4	90.32(6)
H1-O3	1.73 (2)	O3-H1-O4	172.0(14)
H1-O4	0.86 (2)		

3a). The way these units are linked to form the structure (Fig. 3b) resembles that of stishovite, wherein edge-linked octahedra form columns of corner-linked octahedra. In phase egg, H atoms lie in the openings between columns. This efficient packing of H stabilizes this phase, relative to the oxide mixture (SiO_2, Al_2O_3, and H_2O), and other hydroxyl-bearing materials.

Thus, crystal structures of moderate complexity can be determined from high-resolution powder data, even from multiphase mixtures. In addition, the positions of H atoms can be located and refined, as long as the material is highly crystalline and lacks high-Z elements, as they would dominate the scattering.

SCHREINEMAKERS ANALYSIS AND STABILITY OF $AlSiO_3OH$

Experiments conducted on bulk compositions suited to constrain phase relations of phase egg are compiled in Figure 4. Phase egg was synthesized above 700 °C and 12 GPa. Neither its high-pressure nor its high-temperature stability is experimentally determined. The highest pressure at which phase egg was reported is 17.7 GPa at 1200 °C, and the highest temperature is 1300 °C at 15.5 GPa (Irifune et al. 1995). All experiments on phase egg are synthesis experiments and do not necessarily represent equilibrium. However, in a water-saturated system at pressures above 12 GPa and temperatures from 700 to 1300 °C, it appears unlikely that significant differences between synthesis and reversal experiments would occur.

Experiments that resulted in phase egg have been conducted in the chemical systems Al_2O_3-SiO_2-H_2O and CaO-Al_2O_3-SiO_2-H_2O. The stability of the hydrous high pressure silicates (such as topaz-OH and phase egg) are identical for these systems because no phases in the ASH system have a significant Ca-solubility. The experiments compiled in Figure 4 are mutually consistent. The experiment at 1200 °C and 13.5 GPa by Irifune et al. (1995) yielded phase egg + corundum. As seen in Figure 5, this

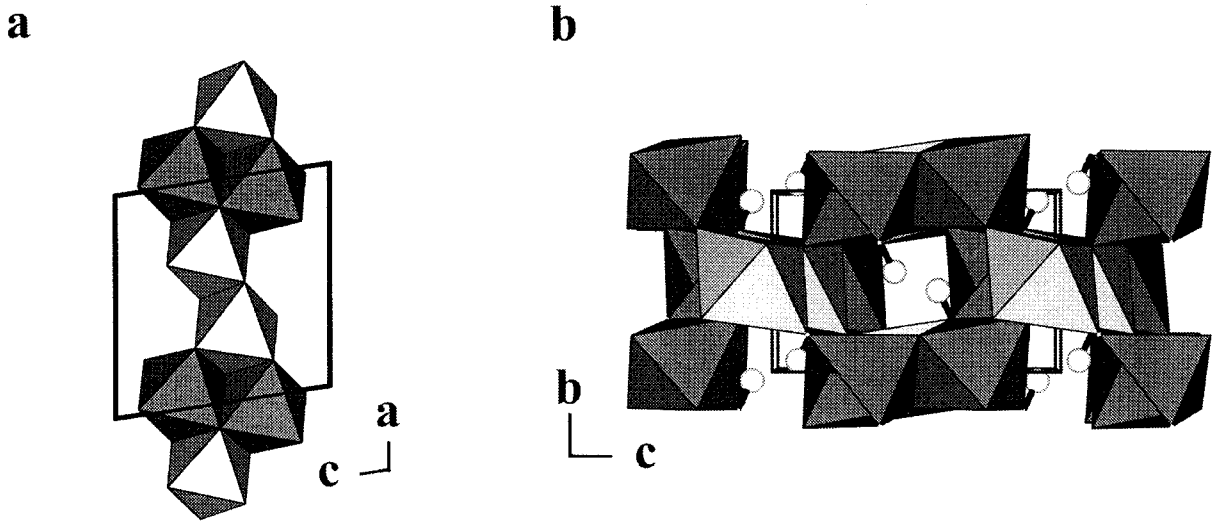

FIGURE 3. Crystal structure of $AlSiO_3OH$. (**a**) The structural module in *a*-*c* projection. (**b**) The linkage of these units in *b*-*c* projection. The diagrams were produced with program DRAWxtl (Finger and Kroeker 1997). Dark octahedra contain Al, bright octahedra Si, the position of the H atom is indicated by white spheres.

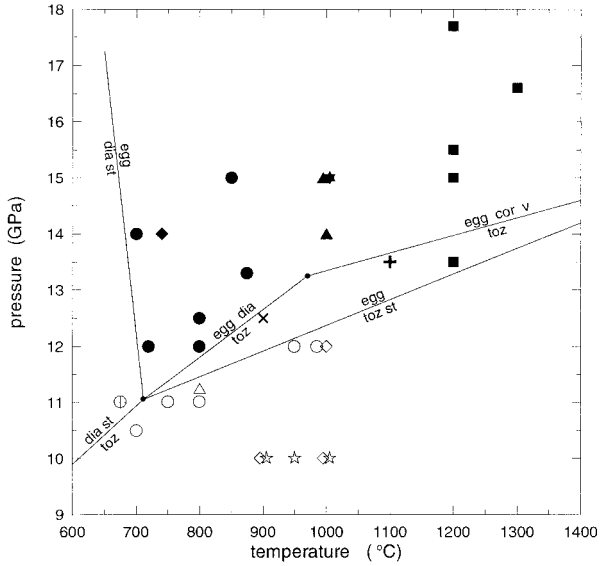

FIGURE 4. Compilation of experiments on bulk composition relevant for the occurrence of phase egg and topaz-OH. Filled symbols = presence of phase egg; open symbols = topaz-OH; crosses = phase egg + topaz-OH; circle with cross = diaspore + stishovite. Triangles and plus sign from this study, open stars from Wunder et al. (1993b), the filled star from Fockenberg et al. (1994), diamonds from Pawley (1994), circles and diagonal cross from Schmidt (1995), squares from Irifune et al. (1995). Abbreviations as follows: $AlSiO_3OH$ (egg), topaz-OH (toz), kyanite (ky), diaspore (dia), corundum (cor), stishovite (st), and vapor (v).

assemblage should be stable at slightly higher pressures (around 13.8 GPa at 1200 °C), however, this pressure difference is largely within the uncertainty of multianvil experiments.

A Schreinemakers analysis of the Al_2O_3-SiO_2-H_2O-system was performed considering the phases egg, topaz-OH, stishovite, corundum, kyanite, diaspore, and vapor. We did not consider melt, however, the temperature stability of phase egg might be delimited by melting reactions and consequently the high-temperature portion of the topologies in Figure 5 would have to be modified. The reactions kyanite = stishovite + corundum (Schmidt et al. 1997), topaz-OH = kyanite + vapor (Wunder et al. 1993b), diaspore = corundum + vapor (Fockenberg et al. 1996; Schmidt 1995) and

$$2\ AlSiO_3OH = 1\ \text{topaz-OH} + 1\ \text{stishovite}, \quad (1)$$

and

$$2\ AlSiO_3OH + 1\ \text{corundum} + 1\ H_2O = 2\ \text{topaz-OH}, \quad (2)$$

and

$$1\ \text{diaspore} + 1\ \text{stishovite} = 1\ AlSiO_3OH \quad (3)$$

are experimentally determined (Fig. 4). These reactions allow one to determine which of the possible homologous grids is stable, and to orient and position these grids in *P-T* space. The extrapolation of d*P*/d*T*-slopes of phase egg and topaz-OH bearing reactions suggest that topaz-

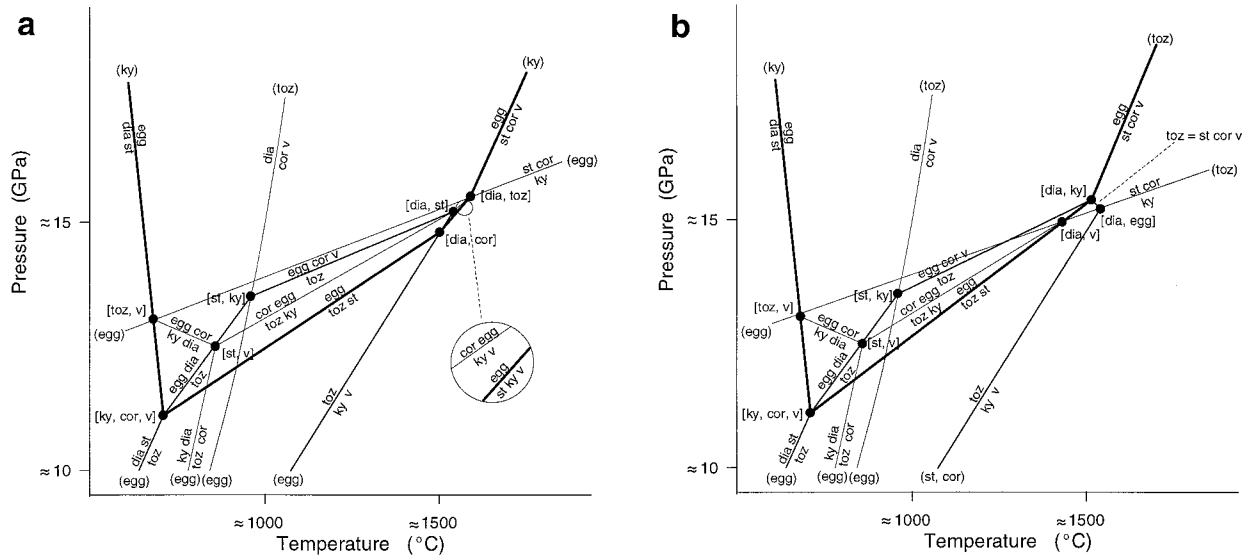

FIGURE 5. Schreinemaker topologies for reactions in the system Al_2O_3-SiO_2-H_2O considering the phases $AlSiO_3OH$, topaz-OH, kyanite, diaspore, corundum, stishovite, and vapor. For abbreviations, see Figure 4. Heavy solid lines delineate approximate stability conditions of phase $AlSiO_3OH$, medium solid lines delineate the upper pressure stability of topaz-OH. The grid is orientated and positioned in *P-T* space according to the experiments in Figure 4 and according to the experimentally determined reactions toz = ky + v (Wunder et al. 1993b), ky = st + cor (Schmidt et al. 1997), and dia = cor + v (Fockenberg et al. 1996; Schmidt et al. 1997). In both grids, two stable invariant points (egg, cor) and (egg, st) locate at pressures below 10 GPa. (**a**) Topology for a breakdown of topaz-OH within the stability field of kyanite. (**b**) Topology for overlapping stability fields of topaz-OH and stishovite + corundum.

OH decomposes within the stability field at kyanite (Fig. 5a). However, given the large uncertainties on the dP/dT-slopes, it might be possible that the stability fields of topaz-OH and of stishovite + corundum overlap. This alternative topology is illustrated in Figure 5b. Our preferred grid (Fig. 5a) differs from the Schreinemaker analysis of the low-pressure stability relations for topaz-OH by Wunder et al. (1993b) in that an intersection of the reactions topaz-OH = kyanite + H_2O and kyanite = coesite + corundum does not occur. The grids of Figure 5 also differs from the Schreinemaker analysis of Pawley (1994): Because the stability field of phase egg extends to temperatures beyond the stability of diaspore, corundum needs to be considered as additional phase to delineate stability relations of phase egg.

The upper pressure stability of topaz-OH and the minimum pressure stability of phase egg is delimited by the following reactions (Figs. 4 and 5a): Phase egg forms from topaz-OH and stishovite according to reaction 1. This reaction has a flat slope of approximately 45 MPa/K in P-T space. Over a limited pressure range (max. 1 GPa), topaz-OH coexists with phase egg until topaz-OH decomposes according to reaction 2 at temperatures above 950 °C. Below approximately 950 °C topaz-OH decomposes through

$$1 \text{ phase egg} + 1 \text{ diaspore} = 1 \text{ topaz-OH} \qquad (4)$$

At low temperatures, phase egg forms around 700 °C according to reaction 3. Estimates yield a subvertical P-T slope for this latter reaction indicating that ΔV of reaction 3 is small although it cannot be accurately determined due to the lack of thermal expansivity and compressibility data for phase egg.

At temperatures and pressures higher than the intersection at reaction 1 with the breakdown reaction of topaz-OH, phase egg decomposes first to stishovite + kyanite + H_2O and then to stishovite + corundum + H_2O (Fig. 5). Both reactions have positive slopes in P-T space, the molar volume of phase egg being significantly lower than the volume of its oxide breakdown products stishovite + corundum + H_2O. It is thus most likely that an unknown, possibly hydrous aluminosilicate, forms instead of phase egg with increasing pressure.

Do high-pressure hydrous aluminosilicates occur in nature?

Phase egg and topaz-OH are potential carriers of water at large depth. Thus we examine bulk compositions and conditions suitable for the occurrence of these phases.

As long as water is present, topaz-OH should occur in eclogites saturated with respect to kyanite, i.e., in peraluminous basalts, in most greywackes, and in metapelites. In fact, topaz-OH was encountered in experiments on metapelites (Domanik and Holloway 1996) at conditions ranging from 6 GPa and 700 °C to 11 GPa and 900 °C. The temperature stability of topaz-OH in these experiments coincides (within the uncertainty resulting from the relatively large thermal gradients in the experiments of Domanik and Holloway 1996) with the end-member reaction in the Al_2O_3-SiO_2-H_2O-system. Toward higher pressures, topaz-OH should react to phase egg through a water conserving reaction. Phase egg with an Al:Si ratio of 1:1 is expected to occur in a wider range of bulk compositions than topaz-OH (Al:Si = 2:1), e.g., phase egg could also appear in metaaluminous bulk compositions such as mid-ocean ridge basalts.

The T-P conditions for the occurrence of topaz-OH and phase egg are characteristic of subduction zones. At pressures of 15 GPa, phase egg was synthesized up to 1300 °C and the maximum temperature stability might be as much as 1500 to 1600 °C. The potential occurrence of phase egg in a wide range of bulk compositions does not necessarily modify significantly the water budget at large depth. At pressures above 12 GPa the nominally anhydrous phases such as clinopyroxene, garnet, olivine, and β-$(Mg,Fe)_2SiO_4$ dissolve significant amounts of H_2O (Bell and Rossmann 1992). Because these phases are at least an order of magnitude more abundant than nominally hydrous phases, the nominally anhydrous phases are expected to be the main carriers of H_2O at depth in excess of 300 km. However, phase egg could be a carrier of water into the deep Earth, owing to its reasonable chemical composition (unlike most of the previously known high-pressure, hydrous silicates, which have very high Mg:Si) and to its high-pressure and high-temperature occurrence.

Acknowledgments

The authors acknowledge the support of the ESRF through grant number CH129, and the help of G. Vaughan in collecting the diffraction pattern. L.W.F. gratefully acknowledges the support of the Alexander von Humboldt Stiftung, Bonn, Germany, and the U.S. National Science Foundation through the Center for High Pressure Research.

References cited

Altomare, A., Cascarano, M.C., Giacovazzo, C., Guagliardi, A., Polidori, C., and Camilli, M. (1994) SIRPOW.92—a program for automatic solution of crystal structures by direct methods optimized for powder data. Journal of Applied Crystallography, 27, 435–436.

Bell, D.R. and Rossman, G.R. (1992) Water in the Earth's mantle: the role of nominally anhydrous minerals. Science, 255, 1391–1397.

Brown, I.D. (1992) Chemical and steric constraints in inorganic solids. Acta Crystallographica, B48, 553–572.

Coes, L. Jr. (1962) Synthesis of minerals at high pressures. In R. Wentdorf, Ed., Modern Very High Pressure Techniques, p. 137–150. Butterworths, London.

de Wolff, P.M. (1968) A simplified criterion for the reliability of a powder pattern indexing. Journal of Applied Crystallography, 1, 108–113.

Domanik, K.J. and Holloway, J.R. (1996) The stability and composition of phengitic muscovite and associated phases from 5.5 to 11 GPa: implications for deeply subducted sediments. Geochimica and Cosmochimica Acta, 60, 4133–4150.

Eggleton, R.A., Boland, J.N., and Ringwood, A.E. (1978) High pressure synthesis of a new aluminum silicate: $Al_5Si_5O_{17}(OH)$. Geochemical Journal, 12, 191–194.

Finger, L.W., Cox, D.E., and Jephcoat, A.P. (1994) A correction for powder diffraction peak asymmetry due to axial divergence. Journal of Applied Crystallography, 27, 892–900.

Finger, L.W. and Kroeker, M. (1997) DRAWxtl—a computer program to generate VRML and POV views of a crystal structure (abstract), ECM–17.

Fockenberg, T., Schreyer, W., Skrok, V., and Wunder, B. (1994) Experimental studies relevant to ultrahigh-pressure metamorphism. Abstract, 16th general meeting of the International Mineralogical Association, Pisa, Italy, p. 121.

Fockenberg, T., Wunder, B., Grevel, K.D., and Burchard, M. (1996) The equilibrium diaspore-corundum at high pressures. European Journal of Mineralogy, 8, 1293–1299.

Irifune, T., Kuroda, K., Minigawa, T., and Unemoto, M. (1995) Experimental study of the decomposition of kyanite at high pressure and high temperature. In T. Yukutake, Ed., The Earth's Central Part: Its Structure and Dynamics, p. 35–44. Terra Scientific Publishing Company, Tokyo.

Katsura, T. and Ito, E. (1989) The system Mg_2SiO_4-Fe_2SiO_4 at high pressures and temperatures: precise determination of the stability of olivine, modified spinel and spinel. Journal of Geophysical Research, 94, 15663–15670.

Larson, A. and Von Dreele, R.B. (1986) GSAS—General Structure Analysis System, Los Alamos National Laboratory Report LA-UR 86-748. Los Alamos, New Mexico.

LeBail, A., Duray, H., and Fourquet, J.L. (1988) Ab-initio structure determination of $LiSbWO_6$ by X-ray powder diffraction. Materials Research Bulletin, 23, 447–452.

Lengauer, C.L., Tillmans, E., Zemann., J., and Robert, J.L. (1995) $Al_2GeO_4(OH)_2$: Rietveld refinement and stereochemical discussion, Zeitschrift für Kristallographie, 210, 656–661.

Pawley, A.R. (1994) The pressure and temperature stability limits of lawsonite: implications for H_2O recycling in subduction zones. Contributions to Mineralogy and Petrology, 118, 99–108.

Rubie, D.C., Karato, S., Yan, H., and O'Neill, H.S.C. (1993) Low differential stress and controlled chemical environment in multianvil high-pressure experiments. Physics and Chemistry of Minerals, 20, 315–322.

Schmidt, M.W. (1995) Lawsonite: Upper pressure stability and formation of higher density hydrous phases. American Mineralogist, 80, 1286–1292.

Schmidt, M.W., Poli, S., Comodi, P., and Zanazzi, P.F. (1997) High pressure behavior of kyanite: Decomposition of kyanite into stishovite and corundum. American Mineralogist, 82, 460–466.

Smith, G.S. and Snyder, R.L. (1979) F_N: a criterion for rating powder diffraction patterns and evaluating the reliability of powder-pattern indexing. Journal of Applied Crystallography, 12, 60–65.

Werner, P.E., Eriksson, L., and Westdahl, M. (1985) TREOR, a semi-exhaustive trial-and-error indexing program for all symmetries. Journal of Applied Crystallography, 18, 367–370.

Wunder, B., Medenbach, O., Krause, W., and Schreyer, W. (1993a) Synthesis, properties and stability of $Al_3Si_2O_7(OH)_3$ (phase Pi) , a hydrous high-pressure phase in the system Al_2O_3-SiO_2-H_2 (ASH) . European Journal of Mineralogy, 5, 637–649.

Wunder, S., Rubie, D.C., Ross, C.R., Medenbach, O., Seifert, F., and Schreyer, W. (1993b) Synthesis, stability, and properties of $Al_2SiO_4(OH)_2$: A fully hydrated analogue of topaz. American Mineralogist, 78, 285–297.

Zhang, J., Li, B., Utsumi, W., and Liebermann, R.C. (1996) In-situ X-ray observation of the coesite-stishovite transition: reversed phase boundaries and kinetics. Physics and Chemistry of Minerals, 23, 1–10.

Manuscript received July 31, 1997
Manuscript accepted January 30, 1998
Paper handled by Lee A. Groat